physica status solidi

pss

www.interscience.wiley.com

reprints

www.pss-rapid.com

www.pss-c.com

www.pss-b.com

www.pss-a.com

WILEY-VCH

REPRINT

Phys. Status Solidi B **247**, No. 6, 1464–1468 (2010) / **DOI** 10.1002/pssb.200983273

physica status solidi b
www.pss-b.com
basic solid state physics

The role of stacking faults and their associated 0.13 eV acceptor state in doped and undoped ZnO layers and nanostructures

K. Thonke*[,1], M. Schirra[1], R. Schneider[1], A. Reiser[1], G. M. Prinz[1], M. Feneberg[1], R. Sauer[1], J. Biskupek[2], and U. Kaiser[2]

[1] Institut für Halbleiterphysik, Universität Ulm, Albert-Einstein-Allee 45, 89069 Ulm, Germany
[2] Materialwissenschaftliche Elektronenmikroskopie, Universität Ulm, Albert-Einstein-Allee 11, 8908169 Ulm, Germany

Received 6 October 2009, revised 27 January 2010, accepted 28 January 2010
Published online 14 April 2010

Keywords cathodoluminescence, crystal defects, nanostructures

* Corresponding author: e-mail klaus.thonke@uni-ulm.de, Phone: +49 731 502 6131, Fax: +49 731 502 6108

Cathodoluminescence spectra recorded with high spatial and wavelength resolution on tilted ZnO epitaxial layers allow to identify a very prominent emission peak at 3.314 eV as a free electron to shallow acceptor ($E_A \approx 130$ meV) transition. By correlation with TEM cross-section images recorded on the same samples we can find these acceptor states to be located on basal plane stacking faults (BSFs). Locally, high concentrations of acceptor states are found. Since this spectral feature is often reported in literature especially after attempts to obtain p-type or transition metal doping, we conclude that stacking faults are a common by-product when group V or other extrinsic atoms are incorporated in ZnO layers or nanostructures.

1 Introduction ZnO layers, bulk crystals, and also nanostructures frequently show an emission band at 3.314 eV in low temperature photoluminescence (PL) measurements, which at room temperature often remains as the dominant spectral PL feature. The band is strong especially after doping with group V elements and is mostly treated as an indicator for successful p-type doping, but also appears in Al-doped ZnO and even in nominally undoped ZnO layers and nanostructures of limited crystal quality. All types of assignments are found for this band: LO- or TO-phonon replicas of free excitons, acceptor-bound excitons (A^0,X), donor–acceptor pair (D^0,A^0) transitions, two-electron satellites (TES), surface-related excitons, or free-to-bound transitions [(e,A^0) or (h,D^0)]. This band is reported to be unstable when annealing is performed.

The correlation of low-temperature cathodoluminescence measurements with very high spatial resolution and high-resolution (HR) transmission electron microscopy (TEM) on the same epitaxial ZnO sample allows us to unambiguously identify this emission band with high-density acceptor states located at c-plane stacking faults (BSFs).

2 Experimental and Results The samples used in this study were 1–3 μm thick ZnO layers with semipolar (−1101) surfaces, *i.e.*, surfaces tilted ≈62° away from the c-plane. The layers were grown by a CVD-like process on a-plane sapphire. The tilted orientation allows to get access to different intersection lines of characteristic crystal planes with the surface and the side walls of the sample, and to distinguish extended crystal defects by their orientation. The CL studies were carried out in a field-emitter scanning electron microscope (LEO DSM 982) equipped with a helium cryostat. Typical electron energies were 2–3 keV allowing for a spatial resolution better than 100 nm. The spectra were recorded with a LN_2 cooled CCD camera mounted to a 0.9 m monochromator [1]. High resolution (HR) TEM were carried out using an FEI Titan 80-300 TEM equipped with a spherical aberration corrector operating at 300 keV. The necessary TEM cross-section samples were prepared using standard techniques such as mechanical grinding and polishing followed by low angle Ar-ion etching.

Figure 1 shows a series of spectra recorded from a 100 μm × 100 μm region on the layer surface. In the bandgap region, at low temperatures the donor bound exciton (D^0,X) dominates, accompanied by a band at ∼3.314 eV.

Upon an increase in the sample temperature, bound excitons are dissociated into free X_A and X_B excitons involving holes in the A or B valence band. The 3.314 eV line

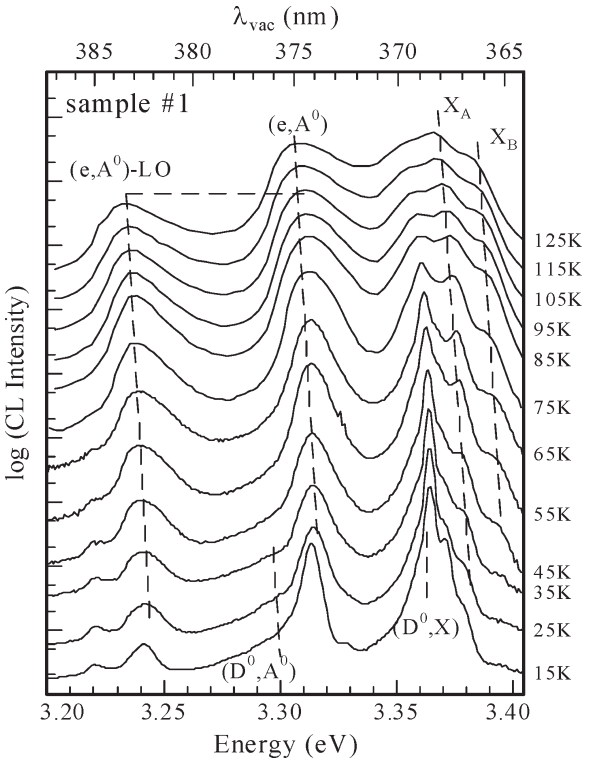

Figure 1 Series of CL spectra from a tilted ZnO layer recorded on an area of ≈100 μm × 100 μm. The (D^0,X) line dominant at 15 K is gradually replaced by free exciton transitions with holes from the A and B valence band involved. At 3.314 eV (*i.e.*, less than an LO energy below the X_A transition) we find the band-acceptor (e,A^0) transition under discussion here. Closer inspection also reveals the associated donor–acceptor (D^0,A^0) recombination.

develops a high energy Boltzmann tail extending more and more toward higher energies for increasing temperatures. Based on quantitative fits we find a purely symmetric Gaussian line shape with ≈5 meV FWHM at low temperature. We ascribe this broadening to the energy distribution of the acceptor states involved. For $T > 25$ K, we have to take into account the density of states of free carriers and the probability, that these states are thermally occupied (approximated by a Boltzmann distribution, since the Fermi level is far enough below the band edge):

$$I(E,T) = \sqrt{E - \left(E_g(T) - E_A\right)}\,\exp(-E/kT). \qquad (1)$$

This line shape has to be convoluted by the Gaussian acceptor energy distribution found for $T = 15$ K, yielding a perfect line shape fit for temperatures up to ∼100 K. For even higher temperatures, a Lorentzian lifetime broadening dominates over the Gaussian distribution changing mainly the shape of the low energy tail [2].

From these line shape fits and knowing the exact bandgap energy from reflectance measurements, the binding energy E_A of the acceptor involved can be derived with very high precision to be $E_A = 130 \pm 2$ meV; the uncertainty is given by the precision of the fit and does not include the superimposed broadening of the acceptor states.

For samples with slightly higher unintentional donor concentration – as mirrored in the higher (D^0,X)/X_A intensity ratio in the PL spectra – we find typically 13–14 meV below the (e,A^0) transition the related donor–acceptor pair transition (D^0,A^0). Whereas in Fig. 1 this transition is rather weak, we find stronger peaks for samples with higher donor concentrations. Knowing the energetic spacing of the (D^0,A^0) from E_{gap}, and the donor concentration (4×10^{17} cm^{-3}) and donor energy (55 meV) from Hall measurements on these samples, we can calculate the average spacing of the D–A pairs: This is 4 nm only, corresponding for homogeneous doping to an acceptor concentration of 4×10^{18} cm^{-3}!

Let us now discuss the microscopic origin of the 3.314 eV transition. To investigate this, we recorded mappings of the wavelength filtered bandgap-near emission on the one hand, and of the 3.31 eV range on the other hand. The selected wavelength ranges are shown by vertical dashed lines in Fig. 2(a). When detecting light either on the top surface or on one of the side facets, we find for most regions the excitonic emission only. Some dark lines interrupt these maps, on which we find the (e,A^0) band instead. Obviously, both transitions compete for free carriers and show total anti-correlation [2]. As an example, the findings on a (11–20) side facet are shown in Fig. 2. The 3.314 eV emission is found along directions perpendicular to the c axis, *i.e.*, on basal c-planes. HRTEM images recorded on the same sample region reveal the existence of two major types of extended defects: basal plane stacking faults (BSFs), and prismatic stacking faults (PSFs), which form the boundaries of the BSFs.

Also for the other surfaces of the sample, we find bright defect emission lines along those directions, which correspond to the intersection of c-planes with the respective surface.

Another interesting piece of information comes from CL spectra recorded locally on ZnO nanopillars (Fig. 3). Defect free regions show only very sharp free and bound exciton lines, whereas obviously imperfect regions mainly emit at 3.314 eV. We conclude from this, that no further extrinsic dopant is required to account for the formation of the defect responsible for the (e,A^0) transition, but that only intrinsic species can lead to the acceptor states.

An open question is the microscopic origin of the 130 meV acceptor states, which are locally present in very high concentration. It seems unlikely, that the stacking faults themselves introduce these levels, since no dangling bonds are expected. A possible candidate is the Zn vacancy, for which ≈180 meV acceptor binding energy is expected [3]. In this case we would have to conclude a reduced formation energy for such Zn vacancies around SFs. Of course, more complicated complexes of intrinsic defects might also be possible.

3 Implications Numerous publications on the PL of ZnO report a band at 3.31 eV with varying and controversial assignments. Quite frequently, this band is observed after

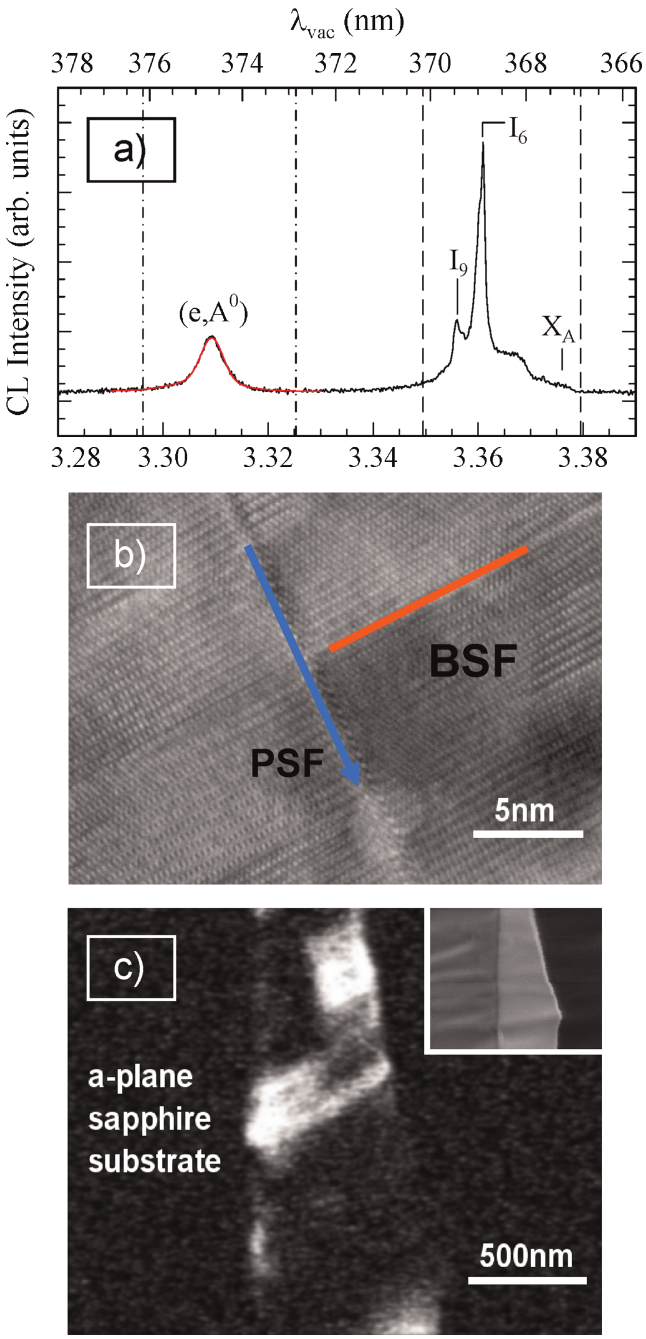

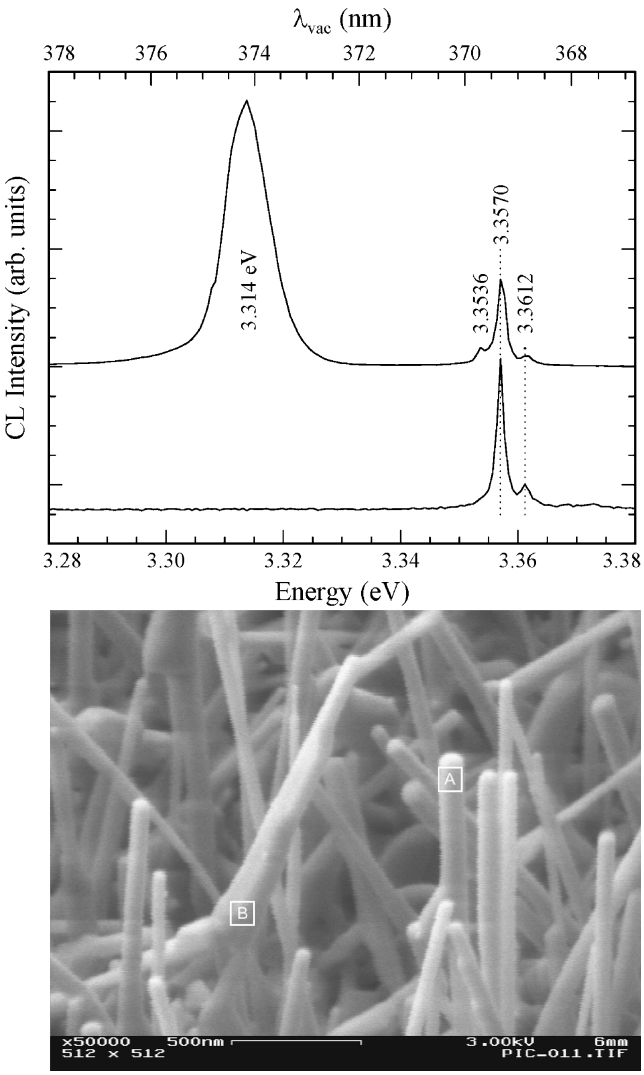

Figure 3 upper figure, lower trace: CL spectrum of a defect free region showing no defects, recorded on the top part of ZnO nanopillars marked by "A" in the lower SEM picture, and (upper trace) a spectrum showing mainly the defect-related 3.314 eV band recorded on a crystallographically ill-defined region marked by "B". Lower figure: SEM micrograph of ZnO pillars on sapphire substrate (tilted view).

Figure 2 (online colour at: www.pss-b.com) (a) Low-temperature ($T \approx 15$ K) CL spectrum drawn to linear scale. Two wavelength ranges marked by vertical dashed lines were selected for the CL mappings: the excitonic range ($E > 3.35$ eV) or the defect related range ($E \approx 3.30$–3.32 eV). The red line is the result of a Gaussian fit. (b) HRTEM image of a (11–20) cross-section through a faceted region of the ZnO layer. BSFs, which are terminated by PSFs are found. The blue arrow also marks the c direction. (c) CL mapping of the defect emission recorded on the same sample region. Whereas the major part of the sample yields luminescence in the excitonic region only and no (e,A^0) signal, some stripes perpendicular to [0001] inversely emit the (e,A^0) band exclusively. Inset: SEM picture of the sample.

intentional p-type doping with group V elements like nitrogen [4, 5], phosphorous [6–8], antimony [9], and arsenic [10]. Expecting that the new PL bands observed after doping must be directly related to the substitutional dopant species, most authors label the 3.31 eV peak as an acceptor bound exciton (A^0,X) or as a donor–acceptor pair transition. We are not aware of any proof (*e.g.*, by Magneto-PL or ODMR), that these assignments are further substantiated. As an alternative explanation we suggest, that a high number of SFs might be created due to the presence of group V atoms during growth, which (over-) compensate the n-type background conductivity and lead to a locally strongly fluctuating Fermi level. Indeed, recent TEM microscopy on such doped samples

finds a high concentration of partial dislocations and stacking faults [11, 12]. However, not only after group V doping this 3.314 eV PL band is found, but also after doping by Mn [13] or doping by Ag [14] introduces this defect band in PL – presumably due to stacking faults introduced in the crystal in high concentration. He et al. [15] report this band also after Al doping of ZnO. But even without intentional doping, bulk crystals can show this PL band to become the dominant emission at temperatures above 100 K [16]. We suspect that in a number of publications this band might have been erroneously ascribed to the 1LO-replica of the free X_A exciton, although the energy spacing is by ≈5 meV too low, and no related free exciton is seen in the spectra – even from very thin nanostructures, where reabsorption cannot totally suppress the X_A emission [17, 18]. Other suggestions are that this band is due to a TO phonon replica of to the X_A, but that the following replicas then should be due to LO phonons [19], without giving any convincing argument of this change in selection rules.

Although it is often expected that stacking faults totally anneal out from nano-sized ZnO structures, we definitely see this PL/CL band from ill-defined regions of ZnO pillars (see Fig. 3). Similarly, the ''DAP1'' transition from nanorods in Ref. [20] might alternatively be explained as SF related emission. TEM images from thin pillars occasionally show this defect [21]. Even the PL spectra recorded on CVD-grown nanoparticles with only 4 nm [22] or 20 nm [23] average diameter are presumably due to the same defect band. Another example of nanostructures, which emit this band, is ''ultra-thin'' nanowires (lying on thicker nanowires) [24]. Although the authors claim that this band is the LO replica of a X_A free exciton up-shifted by quantization effects (while no direct phonon-free X_A transition is observed!), we suggest that this band can alternatively be explained simply by the presence of stacking faults. Feng et al. [25] see a band at 3.31 eV from their nanostructures with varying thickness, which they interpret as a 1LO phonon free exciton replica taking the relative intensity (free exciton – 1LO)/bound exciton as a signature of the volume to surface ratio. Alternatively, simply more stacking faults could occur in the thicker parts. Nanostructures with badly defined side facets might also contain more stacking faults [26].

Several mysteries exist about the p-type doping in ZnO: (i) Most groups find an acceptor activation energy E_A of 110–150 meV from optical or electrical measurements, irrespective of the chemical nature of the acceptor intentionally introduced. (ii) Annealing converts back and forth p-type and n-type conductivity of samples (see, *e.g.*, Ref. [27]). (iii) Hall measurements in van der Pauw configuration give contradictory results when permutating the connections. (iv) Mostly very high dopant concentrations (up to 1%) are necessary to obtain a hole concentration of some 10^{18} cm^{-3} [11]. (v) The carrier mobility of holes is unexpectedly low.

We think, that all these observations can be mostly understood, when in all those experiments reported a large number of stacking faults were generated in parallel. They scatter the carriers, create anisotropic current paths, and create locally a high acceptor concentration. Since the formation energy of SFs is expected to be quite low (≈100 meV only [28]), the pronounced change in concentration upon annealing seems reasonable. Spatially resolved scanning capacitance measurements on group V doped ZnO layers find a correlation between morphological defects and p-type regions embedded in n-type layers [29–31], supporting our assumption.

Acknowledgements C. E. Krill from the University Ulm (Institut für Mikro- und Nanomaterialien) has supported this work with EBSD studies on our ZnO layers. We thank the Kompetenznetzwerk ''Funktionelle Nanostrukturen'' within the ''Landesstiftung'' program of the Federal Government of the State of Baden-Württemberg for financial support.

References

[1] M. Schirra, A. Reiser, G. M. Prinz, A. Ladenburger, K. Thonke, and R. Sauer, J. Appl. Phys. **101**, 113509 (2007); J. Virtual Nanoscale Sci. Technol. **15**, No. (24), (2007).
[2] M. Schirra, R. Schneider, A. Reiser, G. M. Prinz, M. Feneberg, J. Biskupek, U. Kaiser, C. E. Krill, K. Thonke, and R. Sauer, Phys. Rev. B **77**, 125215 (2008).
[3] A. Janotti and C. G. Van de Walle, Appl. Phys. Lett. **87**, 122102 (2005).
[4] D. C. Look, D. C. Reynolds, C. W. Litton, R. L. Jones, D. B. Eason, and G. Cantwell, Appl. Phys. Lett. **81**, 1830 (2002).
[5] E. Przezdziecka et al., Semicond. Sci. Technol. **22**, 10 (2007).
[6] F. X. Xiu, Z. Yang, L. J. Mandalapu, and J. L. Liu, Appl. Phys. Lett. **88**, 152116 (2006).
[7] J. D. Ye, S. L. Gu, F. Li, S. M. Zhu, R. Zhang, Y. Shi, Y. D. Zheng, X. W. Sun, G. Q. Lo, and D. L. Kwong, Appl. Phys. Lett. **90**, 152108 (2007).
[8] D.-K. Hwang, M.-S. Oh, Y.-S. Choi, and S.-J. Park, Appl. Phys. Lett. **92**, 161109 (2008).
[9] E. Przézdziecka, E. Kaminska, I. Pasternak, A. Piotrowska, and J. Kossut, Phys. Rev. B **76**, 193303 (2007).
[10] J. M. Erie, M. Ivill, H. S. Kim, S. J. Pearton, B. Gila, F. Ren, and D. P. Norton, Phys. Status Solidi A **205**, 1647 (2008).
[11] W. Guo, A. Allenic, Y. B. Chen, X. Q. Pan, Y. Che, Z. D. Hu, and B. Liu, Appl. Phys. Lett. **90**, 242108 (2007).
[12] A. Allenic, W. Guo, Y. Chen, M. B. Katz, G. Zhao, Y. Che, Z. Hu, B. Liu, S. B. Zhang, and X. Pan, Adv. Mater. **19**, 3333 (2007).
[13] M. Diaconu, H. Schmidt, H. Hochmuth, M. Lorenz, G. Benndorf, J. Lenzner, D. Spemann, A. Setzer, K.-W. Nielsen, P. Esquinazi, and M. Grundmann, Thin Solid Films **486**, 117 (2005).
[14] H. S. Kang, B. D. Ahn, J. H. Kim, G. H. Kim, S. H. Lim, H. W. Chang, and S. Y. Lee, Appl. Phys. Lett. **88**, 202108 (2006).
[15] H. P. He, H. P. Tang, Z. Z. Ye, L. P. Zhu, B. H. Zhao, L. Wang, and X. H. Li, Appl. Phys. Lett. **90**, 023104 (2007).
[16] D. W. Hamby, D. A. Lucca, M. J. Klopfstein, and G. Cantwell, J. Appl. Phys. **93**, 3214 (2003).
[17] H. Fan, C. Y. Zhu, S. Fung, Y. C. Zhong, K. S. Wong, Z. Xie, G. Brauer, W. Anwand, W. Skorupa, C. K. To, B. Yang, C. D. Beling, and C. C. Ling, Small **2**, 561 (2006).
[18] T. Yatsui, J. Lim, T. Nakamata, K. Kitamura, M. Ohtsu, and G.-C. Yi, Nanotechnology **18**, 065606 (2007).

[19] Y. Zhang, B. Lin, X. Sun, and Z. Fu, Appl. Phys. Lett. **86**, 131910 (2005).
[20] B. P. Zhang, N. T. Binh, Y. Segawa, K. Wakatsuki, and N. Usami, Appl. Phys. Lett. **83**, 1635 (2003).
[21] M. C. Jeong, S.-W. Lee, J.-M. Seo, and J.-M. Myoung, Nanotechnology **18**, 305701 (2007).
[22] V. A. Fonoberov, K. A. Alim, A. A. Balandin, and F. Xiu, Phys. Rev. **B73**, 165317 (2006).
[23] L. Schneider, S. V. Zaitsev, G. Bacher, W. Jin, and M. Winterer, J. Appl. Phys. **102**, 023524 (2006).
[24] D. Stichtenoth, C. Ronning, T. Niermann, L. Wischmeier, T. Voss, C.-J. Chien, P.-C. Chang, and J. G. Lu, Nanotechnology **18**, 435701 (2007).
[25] L. Feng, C. Cheng, B. D. Yao, N. Wang, and M. M. T. Loy, Appl. Phys. Lett. **95**, 053113 (2009).
[26] W. Kwok, A. B. Djurišic, Y. H. Leung, W. K. Chan, D. L. Phillips, H. Y. Chen, C. L. Wu, S. Gwo, and M. H. Xie, Chem. Phys. Lett. **412**, 141 (2005).
[27] A. Allenic, W. Guo, Y. Chen, M. B. Katz, G. Zhao, Y. Che, Z. Hu, B. Liu, S. B. Zhang, and X. Pan, Adv. Mater. **19**, 3333 (2007).
[28] Y. Yan, G. M. Dalpian, M. M. Al-Jassim, and S.-H. Wei, Phys. Rev. B **70**, 193206 (2004).
[29] H. v. Wenckstern, G. Benndorf, S. Heitsch, J. Sann, M. Brandt, H. Schmidt, J. Lenzner, M. Lorenz, A. Y. Kuznetsov, B. K. Meyer, and M. Grundmann, Appl. Phys. A **88**, 125 (2007).
[30] B. Wang, J. Min, Y. Zhao, W. Sang, and C. Wang, Appl. Phys. Lett. **94**, 192101 (2009).
[31] A. Krtschil, A. Dadgar, N. Oleynik, J. Bläsing, A. Diez, and A. Krost, Appl. Phys. Lett. **87**, 262105 (2005).

